

Biochemical properties and mechanism of action of a vanadyl(IV) – aspirin complex on bone cell lines in culture

Susana B. Etcheverry^{1,2,*}, Patricia A.M. Williams², Viviana C. Sállice¹, Daniel A. Barrio¹, Evelina G. Ferrer² & Ana M. Cortizo¹

¹*Bioquímica Patológica*, ²*CEQUINOR (Centro de Química Inorgánica, UNLP-CONICET), Facultad de Ciencias Exactas, Universidad Nacional de La Plata. 47 y 115 (1900) La Plata, Argentina; *Author for correspondence*

Received 12 March 2001; accepted 12 June 2001

Key words: aspirin, cytotoxicity, osteoblasts, vanadium

Abstract

A recently synthesized vanadyl(IV) complex with aspirin [VO(aspirin)ClH₂O]₂, has been thoroughly investigated by physicochemical techniques. In order to support the proposed structure, stoichiometry and the coordination sphere of the vanadium center, some studies such as elemental analysis, electronic (diffuse reflectance) and vibrational (infrared) spectroscopies, magnetic susceptibility, as well as the thermal behavior, were carried out. The bioactivity of the vanadium complex (VOAspi) was evaluated on two osteoblast-like cell lines in culture, being its cytotoxic effects stronger than the vanadyl cation as assessed by morphological changes and lipid peroxidation. These effects may be partially explained through the induction of the expression of Erks (Extracellular signal-regulated kinases) and the inhibition of the PTPases (Phosphotyrosine phosphatases) present in the cellular extracts.

Introduction

Vanadium is a trace transition metal with relevant biological properties since it can interact with different biomolecules in its anionic and cationic forms (Chasteen 1990). Our interest in the coordination chemistry and biological effects of vanadium compounds has been stimulated by the discovery of its insulin mimetic properties and potential therapeutic applications (Shechter 1990; Srivastava & Chiasson 1995). For instance, vanadium regulates the glucose level in the blood of diabetic laboratory animals and diabetic patients (Stern *et al.* 1993; Goldfine *et al.* 1998). It modulates cellular metabolic processes such as glucose uptake and glucose oxidation, lipid metabolism, and also proliferative events like mitogenesis and cellular differentiation. However, high doses and chronic treatment with vanadium can cause toxic effects (Domingo 2000). Even though the precise mechanism involved in the biological effects of vanadium compounds is still uncertain, experimental data support the hypothesis that these compounds ex-

ert their actions by regulating the cellular levels of tyrosine phosphorylation. Vanadium derivatives may, indirectly, enhance the levels of tyrosine phosphorylated proteins by inhibiting protein tyrosine phosphatases (PTPases) (Gresser & Tracey 1990; Krejsa *et al.* 1997), subsequently inducing many biological effects. On the other hand, when vanadium enters the organism of vertebrates through the gastrointestinal and respiratory tracts, is absorbed by and distributed throughout the tissues, being mainly accumulated in bones, kidneys and liver (Etcheverry & Cortizo 1998; Nriagu 1998). Moreover, it has been previously reported that vanadium deficiency causes impaired growth and skeletal deformations (Nielsen 1995).

Aspirin, a compound that is largely produced by the pharmaceutical industry, is used as an effective antipyretic, analgesic and antiinflammatory drug. Copper complexes of antiinflammatory drugs have been found to be more potent and desirable than the parent ligands themselves (Brown *et al.* 1980; Sorenson 1982). Preliminary results of the synthesis and physicochemical characterization of a new

vanadyl(IV)/aspirin complex (VOAspi) as well as its biological effects on bone related cells, were previously and partially reported (Etcheverry *et al.* 2000). In osteoblast-like cells, vanadium(IV) caused a slight but statistically significant increase in cell proliferation, VOAspi being more potent than vanadyl cation. However, at high concentrations both compounds inhibited MC3T3E1 non transformed cells, while only VOAspi caused a cytotoxic effect on UMR106 osteosarcoma cells. The VOAspi complex induced a dose-dependent decrease in the osteoblast differentiation as assessed by alkaline phosphatase activity (ALP).

The aims of this study were to analyze the magnetic and thermogravimetric properties of VOAspi as well as to study in detail its infrared and diffuse reflectance spectra. Also, the cytotoxic effects and the possible mechanism involved in VOAspi bioactivity were further evaluated in osteoblast-like cells in culture.

Materials and methods

Materials

Vanadium(IV) oxide sulfate (vanadyl sulfate) was provided by Merck (Darmstadt, Germany), VOCl_2 (Carlo Erba) 50% aqueous solution was used without further purification. Acetylsalicylic acid (Aspirin) was provided by SIGMA Chemical Co. (St. Louis, Missouri). Tissue culture material was from Corning (Princeton, New Jersey), Dulbecco's Modified Eagles Medium (DMEM), trypsin-EDTA (ethylenediaminetetraacetic acid) from Gibco (Gaithersburg, Maryland) and fetal bovine serum (FBS) from Gen (Argentina). All other chemicals used were of analytical grade from Sigma.

Rabbit polyclonal anti-Erks (extracellular signal-regulated kinases) antibody was from Santa Cruz Biotechnology (Santa Cruz, California). Biotin conjugated antirabbit polyclonal antibody, avidin-alkaline phosphatase and substrate solution: 5-Bromo-4-chloro-3-indolyl phosphate (BCIP) plus nitroblue tetrazolium (NBT) were from Vectastain (ABC kit, Vector Laboratories Inc., Burlingame, California).

VOAspi was synthesized as previously reported (Etcheverry *et al.* 2000).

Physicochemical characterization of VOAspi

Diffuse reflectance spectrum was measured on a Shimadzu UV-300 spectrophotometer, with MgO as standard.

Infrared (IR) spectra were recorded on a Perkin-Elmer 580B spectrophotometer. The solid complex was measured using the KBr technique.

Room temperature magnetic susceptibility was determined with a Cahn-2000 balance, calibrated with $\text{Hg}[\text{Co}(\text{SCN})_4]$ and at a magnetic field strength of 6 kG.

Thermogravimetric (TG) and differential thermal analysis (DTA) were performed on a Shimadzu thermoanalytical system (models TG 50 and DTA 50). Alumina was used as a DTA standard. Measurements were performed under an oxygen flow (60 ml min^{-1}) using Pt-crucibles at a heating rate of $10 \text{ }^\circ\text{C min}^{-1}$.

Cell culture

Osteoblastic non transformed mouse calvaria (MC3T3E1) and rat osteosarcoma (UMR106) derived cells were grown in DMEM supplemented with 100 U ml^{-1} penicillin, $100 \text{ } \mu\text{g ml}^{-1}$ streptomycin and 10% (v/v) FBS at $37 \text{ }^\circ\text{C}$, 5% CO_2 . When 70–80% confluence was reached, cells were subcultured using 0.1% trypsin – 1 mM EDTA in Ca^{+2} – Mg^{+2} free phosphate buffered saline (PBS) (Cortizo & Etcheverry 1995, Etcheverry *et al.* 1997). In our experiments, cells were grown in six-well plates at a density of 2.5×10^4 cells well^{-1} . When cells reached 70% confluence, the monolayers were washed twice with DMEM. Cells were incubated overnight with vanadium compounds at different doses in serum free DMEM. In order to test the biological effects, fresh stock solutions of vanadyl(IV) sulfate or VOAspi were prepared with distilled water at 10 or 100 mM concentration as it was previously described (Etcheverry *et al.* 1997; Etcheverry *et al.* 2000).

Whole-cell homogenate and cell fraction preparation

MC3T3E1 osteoblast-like cells were grown to confluency in 150 cm^2 flasks. Cells were washed with PBS, resuspended in a homogenizing buffer (25 mM Tris, 250 mM sucrose, 2 mM EDTA, 5 mM β -mercaptoethanol, 1 mM phenyl-methyl-sulphonyl-fluoride (PMSF), pH 7.4), and sonicated three times for 60 s. The homogenate was centrifuged at $1,000 \times g$ for 10 min, and supernatant was further centrifuged at $10,000 \times g$ at $4 \text{ }^\circ\text{C}$ for 30 min. Membranes were

then isolated from the supernatant by centrifugation at $105,000 \times g$ for 60 min at 4 °C. The resulting pellet was solubilized in 0.1% Triton X-100/PBS. Protein concentration in both supernatant and membrane fractions was determined by the Bradford's (1976) method. This material was stored at -20 °C until PTPase activity was determined.

Cytotoxicity

Cells growing into six well plates were incubated overnight with vanadium compounds in serum-free DMEM or media alone (control or basal condition). After two washes with PBS, monolayers were fixed with methanol for 5 min at room temperature and stained with 1:10 dilution of Giemsa for 10 min. Finally, plates were washed with water and morphological changes induced by vanadium compounds were observed by light microscopy (Sállice *et al.* 1999).

Lipid peroxidation. TBARS (Thiobarbituric acid reactive species) production

To measure the extent of lipid peroxidation, TBARS production was evaluated as it was previously described (Cortizo *et al.* 2000a), by using Ohkawa's (1979) method. Cell extract protein content was assessed by Bradford's (1976) method. Lipid peroxide levels were expressed in terms of nmol of malondialdehyde produced per mg protein, using 1,1,3,3-tetramethoxypropane as standard.

Detection of Erks by western blot

After incubation with or without vanadium derivatives, cells were washed with cold PBS pH 7.4, scraped in the sample buffer [0.0625 M tris(hydroxymethyl)-aminomethane (Tris) - HCl, pH 6.8, 2% SDS, 5% 2-mercaptoethanol, 0.001% bromophenol blue, 10% glycerol] and boiled for 5 min (Laemmli 1970). Then, 50 μ l of the extract (corresponding to 100 μ g protein) were subjected to electrophoresis on 12.5% sodium dodecylsulfate (SDS) - polyacrylamide gels (PAGE). A sample corresponding to basal condition was included in each experiment. Then, proteins were transferred onto nitrocellulose overnight at 70 mA. Immunological determinations were performed using rabbit polyclonal anti-Erk as primary antibody. In order to control loading and transfer, the membranes were reversibly stained with 0.2% Ponceau S in 3% trichloroacetic acid before the blocking (Cortizo *et al.* 2000b). After 3 washes with water, filters were

blocked by incubation with 3% non-fat milk in PBS (pH 7.4) for 30 min at room temperature. Antibody binding was performed in TBS (Tris-buffered saline) with 1% bovine serum albumin (BSA), overnight at 4 °C, using a 1:500 dilution. Filters were washed four times with PBS for 15 min and incubated with biotinylated antirabbit second antibody (1:2,000) in TBS-1% BSA for 30 min at room temperature. After washing them four times with PBS, nitrocellulose was incubated with avidin-alkaline phosphatase for 30 min at room temperature and then washed four times with PBS. Visualization was performed by incubating the filters with alkaline phosphatase substrates NBT-BCIP until the color developed.

PTPases activity measurement

This activity was estimated by the potency of cell extract (50 μ g protein ml^{-1}) to hydrolyze *p*-nitrophenyl phosphate (pNPP) according to Li *et al.* (1996). The assay (final volume 1 ml) consisted of 5 mM pNPP in 50 mM HEPES (N-(2-hydroxyethyl)-piperazine-N'-(2-ethanesulfonic acid)), pH 7.5, enzyme source and different concentrations (0-100 μ M) of vanadium compounds. After 30 min of incubation period, optical density was measured at 405 nm. In addition, the effects of vanadium compounds on the alkaline PTPase present in the cell extract were also assayed by using a glycine buffer pH 10.5.

Statistical analysis

At least three independent experiments were performed by triplicate for each experimental condition. Data were expressed as mean \pm SEM ($n = 9$). Statistical differences were analyzed using Student's *t*-test.

Results and discussion

Physicochemical properties of VOAspi

In order to obtain a deeper insight into the physicochemical properties of the VOAspi complex, the following determinations were performed:

Elemental analysis

Calc. for $\text{C}_{18}\text{H}_{18}\text{Cl}_2\text{O}_{12}\text{V}_2$ (599): C, 36.00; H, 3.00; V, 17.03; Cl, 11.85. *Found:* C, 36.26; H, 3.16; V, 16.95; Cl, 12.05%.

Table 1. Characteristic IR vibrations for Aspirin and VOAspi.

Aspirin (cm ⁻¹)	VOAspi (cm ⁻¹)	Assignments
2984 m	2980 m	$\nu_{\text{as}}\text{CH}_3$
2940 m	2933 m	$\nu_{\text{as}}\text{CH}_3$
2910 m	2908 m	$\nu_{\text{s}}\text{CH}_3$
1754 s	1768 sh	$\nu\text{C}=\text{O}$ ($-\text{C}(\text{O})\text{OCH}_3$), Fermi
	1745 s	resonance (see text)
1690 vs		$\nu\text{C}=\text{O}$ ($-\text{COOH}$)
	1592 s	δOH_2
	1537 s	$\nu_{\text{as}}\text{COO}^-$
1482 w	1482 w	$\delta^{\text{IP}}\text{PhH}$, νCC , $\tau\text{H}_3\text{CCO}$, $\delta_{\text{as}}\text{CH}_3$
1458 s	1450 m	$\tau\text{H}_3\text{CCO}$, $\delta_{\text{as}}\text{CH}_3$
1419 m	See text	$\delta_{\text{s}}\text{CH}_3$
	1403 vs	$\nu_{\text{s}}\text{COO}^-$
1305 vs	1297 vw	$\nu\text{C}-\text{O}$ ($-\text{COOH}$)
	988 s	$\nu\text{V}=\text{O}$

vs = very strong, s = strong, m = medium, w = weak, vw = very weak, sh = shoulder.

Diffuse reflectance

The spectrum of the solid complex presents two broad and not well-defined bands at 810 and 610 nm. This pattern agrees with that of VOAspi in solution (Etcheverry *et al.* 2000). The shift of the two typical bands of the free vanadyl(IV) cation (Ballhausen & Gray 1962; Lever 1984) to red and blue, respectively, suggests coordination of this metal through the carboxylate groups of the ligand (Johnson & Shepherd 1978; Ferrer *et al.* 1993; Kögerler *et al.* 1996; Williams *et al.* 1998; Allegretti *et al.* 2000). As the position of the electronic absorption bands either in solution or in solid state are found to be quite similar, it can be assumed that the structure of the solid complex is retained upon dissolution.

Infrared (IR) spectroscopy

Table 1 shows the characteristic vibrations for Aspirin and VOAspi complex. The IR spectrum of Aspirin has been assigned according to previous reported data (Binev *et al.* 1990). The bands at 2984 and 2940 cm⁻¹, corresponding to the antisymmetric stretching of the methyl group, remain unchanged in the VOAspi complex. A similar result was observed with the ν_{s} vibration of this group. The C=O stretching band at 1754 cm⁻¹ presents a clearly defined shoulder in the complex, probably due to Fermi resonance. These features indicate that the acetyl group remains intact upon complex formation. This behavior is different from that observed in the case of uranyl (UO₂²⁺), Bi³⁺ and

Zn²⁺ complexes of the acetylsalicylic acid in which the coordination takes place through the carboxylic and the acetyl groups (Baslas *et al.* 1979). On the other hand, the carboxylic group stretching band of the ligand is replaced by two vibrations corresponding to the antisymmetric and symmetric stretchings of the carboxylate group in the complex. The free aspirinate anion presents a $\Delta[\nu_{\text{as}}(\text{CO}_2^-) - \nu_{\text{s}}(\text{CO}_2^-)] = 239 \text{ cm}^{-1}$. The Δ value for VOAspi is 134 cm⁻¹, indicating that the carboxylate groups behave as bidentate ligands, suggesting the formation of a binuclear species (Carvill *et al.* 1989; Lin-Vien *et al.* 1991; Nakamoto 1997).

The band of the complex located at 1592 cm⁻¹ has been assigned to the bending vibration of the water molecule since it disappears by heating at 140 °C. Moreover, in the complex, the strong and broad symmetric stretching band of the carboxylate group masks the symmetric bending of the methyl group placed at 1419 cm⁻¹ in the Aspirin spectrum.

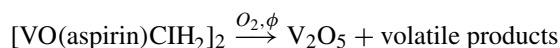
On the other hand, another remarkable change occurs with the C-O stretching band of the carboxylic acid (1305 cm⁻¹, vs) (Lin-Vien *et al.* 1991). It can be observed a slight frequency shift and a strong intensity decrease through coordination to the vanadyl(IV) cation. Moreover, the V=O stretching is observed as a new and strong band at 988 cm⁻¹.

Magnetic susceptibility (room temperature): 1.34 BM per vanadium atom

This subnormal magnetic moment value may be due to an antiferromagnetic exchange between the d¹ electron of each metallic center of the dimer. In addition, the presence of bridging carboxylate groups may force vanadium ions to come close together. Exchange interactions may then occur by Π overlap of the vanadium d_{xy} orbital with the Π symmetry orbitals of the COO⁻ groups (Syamal 1975).

Thermal behavior

A typical thermogram under an oxygen flow is shown in Figure 1. As can be seen, two successive degradation steps are observed (67 °C and 167 °C). At 210 °C the complex has given up nearly 18.4% of its mass, which corresponds to the loss of ca. 2 moles of water and 2 moles of HCl (calculated = 18.2%). The last two steps, which are extended up to 400 °C, are related to the exo DTA-peaks located at 260 and 355 °C. Total thermal degradation can be represented by the following equation:



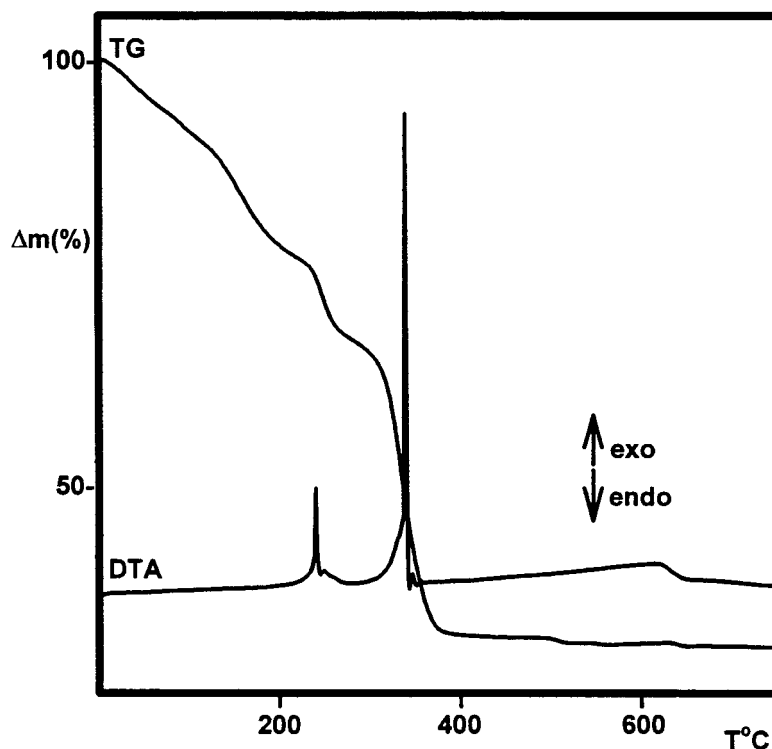


Fig. 1. TG and DTA curves for the solid $[\text{VO}(\text{aspirin})\text{ClH}_2\text{O}]_2$ complex. O_2 flow: 60 ml/min; heating rate: $10^\circ\text{C min}^{-1}$

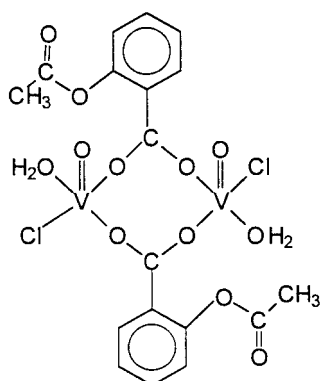


Fig. 2. Proposed structure for VOAspi complex.

The residual mass found was 30.8%, which is in agreement with the theoretical value of 30.4%. The generation of V_2O_5 as the only solid residue was confirmed by IR spectroscopy. On the other hand, the weak endothermic peak observed in the thermogram at ca. 650°C quite agrees with the fusion temperature of V_2O_5 (658°C) (Clark 1973). The proposed stoichiometry and composition of the VOAspi complex has also been confirmed by the results of the thermal analysis.

The structure shown in Figure 2 can be suggested on the basis of the physicochemical studies. It can be seen that each vanadium(IV) atom of the dimer shows a square pyramid as its coordination sphere. Each vanadium(IV) coordinates with the oxygen atom of the vanadyl group, two oxygens from the carboxylate bridging groups, one oxygen from the water molecule and one chloride anion.

Cytotoxic effects

As we have previously reported (Barrio *et al.* 1997; Etcheverry *et al.* 1997; Sállice *et al.* 1999), vanadium compounds induced morphological changes in MC3T3E1 cells. These cells show (Figure 3A) a fibroblastic shape with multiple processes connecting each other and also well defined nuclei with nucleoli. The effects of $10\ \mu\text{M}$ VO in MC3T3E1 cells after 24 h incubation such as changes in the normal phenotype, as the loss of some intercellular connections and condensation of cytoplasm, can be seen in Figure 3B. More pronounced alterations with similar characteristics were induced by VOAspi (Figure 3C). These observations parallel the effect of these vanadium compounds on cell proliferation (Etcheverry

et al. 2000) and suggest a stronger cytotoxic effect of VOAspi in comparison with the vanadyl(IV) cation.

Mechanism of action of VOAspi: Lipid peroxidation

The role of the oxidative mechanisms in the vanadium-induced cytotoxicity was evaluated in the osteoblast-like cells by assessing TBARS formation. Figure 4A and B show that VO and VOAspi increased lipid peroxidation in a concentration-dependent manner. In both cell lines, UMR106 and MC3T3E1, VOAspi was more potent than VO at doses lower than 2.5 mM.

We have previously shown (Cortizo *et al.* 2000a) that vanadate-induced cytotoxicity is partially dependent on oxidative stress. A negative correlation was found between cell survival and TBARS formation. In this study, we have also observed that there is an association between TBARS level induced by VOAspi and its cytotoxic effects, suggesting a role for the lipid peroxidation in the VOAspi mechanism of action.

Effect of vanadium on Erk-1 and Erk-2 expression

Vanadium compounds inhibit PTPases and consequently prevent dephosphorylation and cause a rapid increase in the phosphorylation of tyrosine residues of multiple proteins. Like insulin, vanadium induces the phosphorylation and activation of docking molecules like IRS-1 and Src, leading in turn to activation of the signaling cascade of the mitogen activated protein kinases (MAPK) (White & Kahn 1994; Pandey *et al.* 1999).

In osteoblast-like cells, vanadium compounds promote the tyrosine phosphorylation of several proteins (Sálice *et al.* 1999). To examine whether the expression of Erks is regulated by vanadium, Erk-1 and -2 were analyzed by Western blot. UMR106 osteoblast-like cells were treated with VO and VOAspi during different incubation periods (Figure 5). Both compounds induced the expression of Erk-1 and -2, detected as 44- and 42-kDa proteins, in a time-dependent manner (Figure 5A and B). The quantification of these bands showed the highest stimulation between 10 and 30 min for VO and VOAspi (Figure 5C and D). The treatment with VO and VOAspi for 10 min increased the expression of Erk-1 and -2 in a dose-response manner (Figure 6A and B). The expression of Erks was dependent on the concentration of vanadium, attaining its maximum between 250–500 μ M for both compounds (Figure 6C and D).

In the non-transformed MC3T3E1 cells, VO and VOAspi caused a time- and dose-response induction

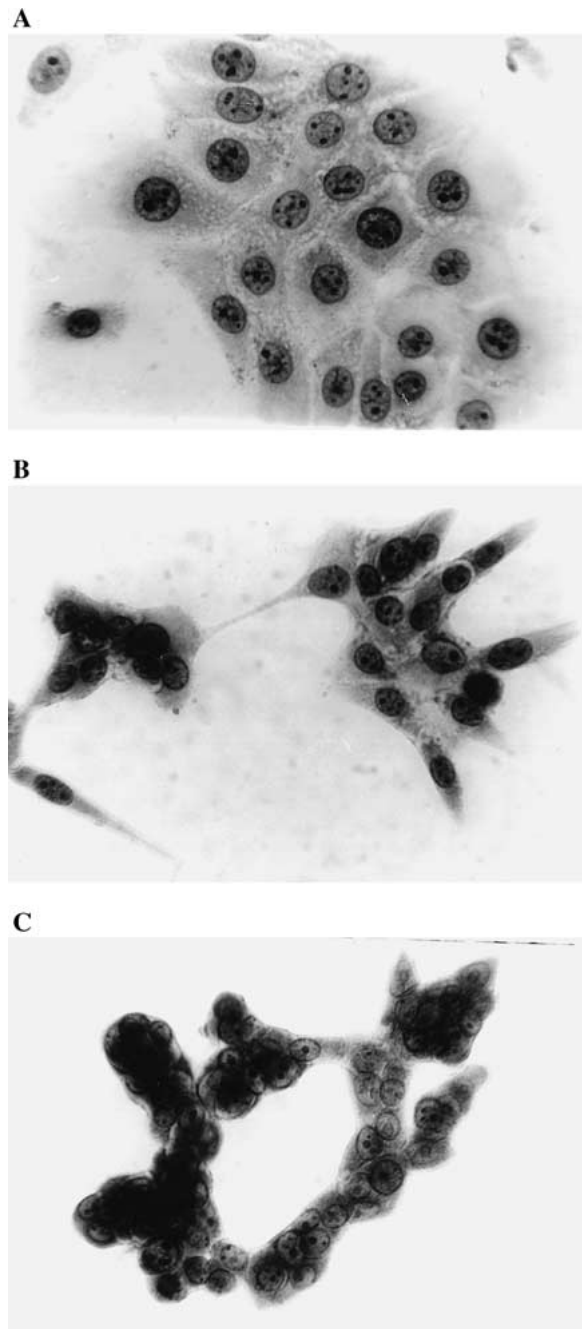


Fig. 3. Effect of vanadium compounds on MC3T3E1 cell morphology. Osteoblasts were incubated in serum free DMEM without addition (A), with 10 μ M vanadyl (B) or with 10 μ M VOAspi (C). Cells were stained with Giemsa. Obj. 40X.

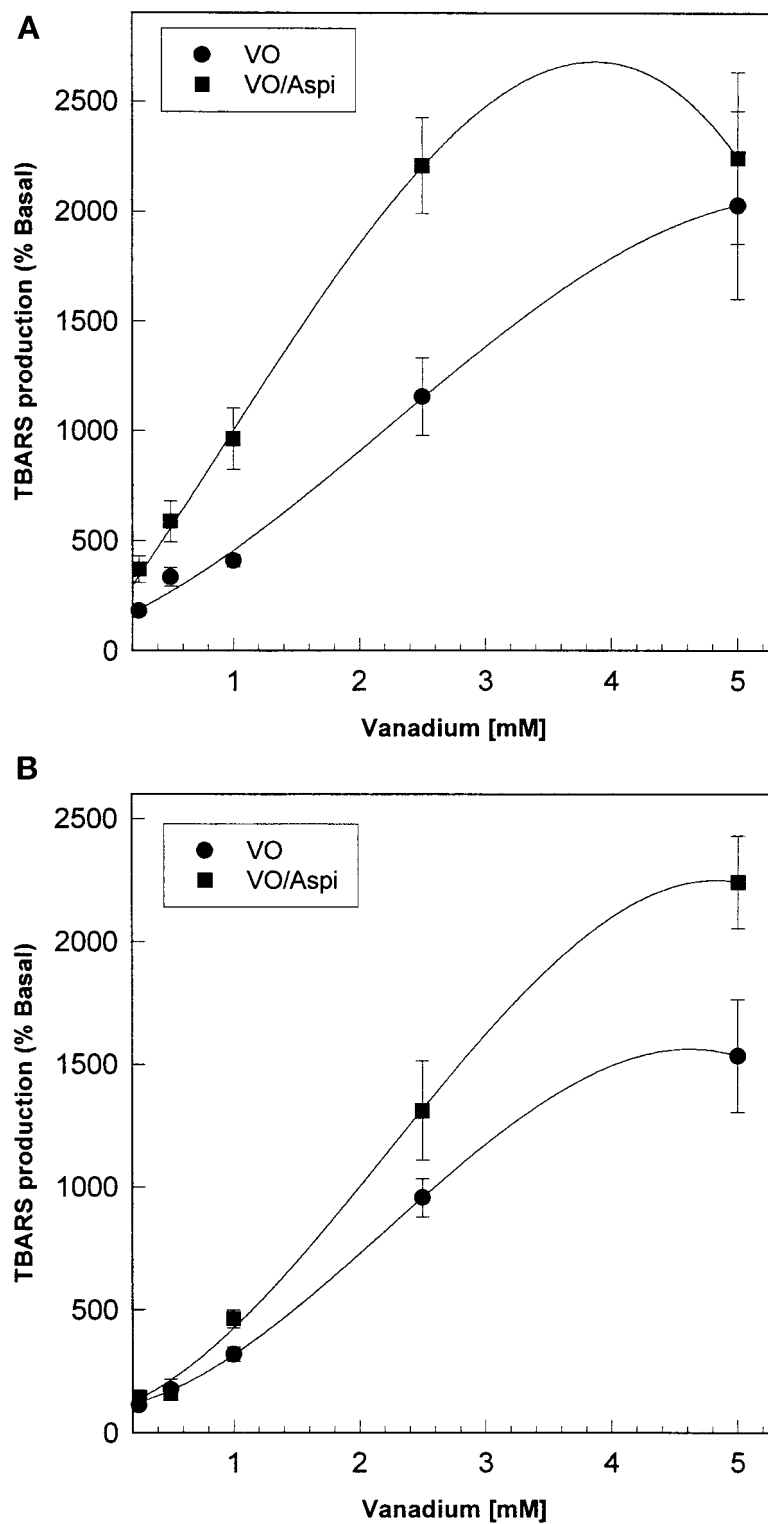


Fig. 4. Vanadium induced-lipid peroxidation in UMR106 (A) and MC3T3E1 (B) osteoblast-like cells. Cells were incubated in a serum-free DMEM with or without different vanadium concentrations at 37 °C for 4 h. TBARS was assessed as described in *Material and Methods*. Results are expressed as % basal and represent the mean \pm SEM ($n = 6$).

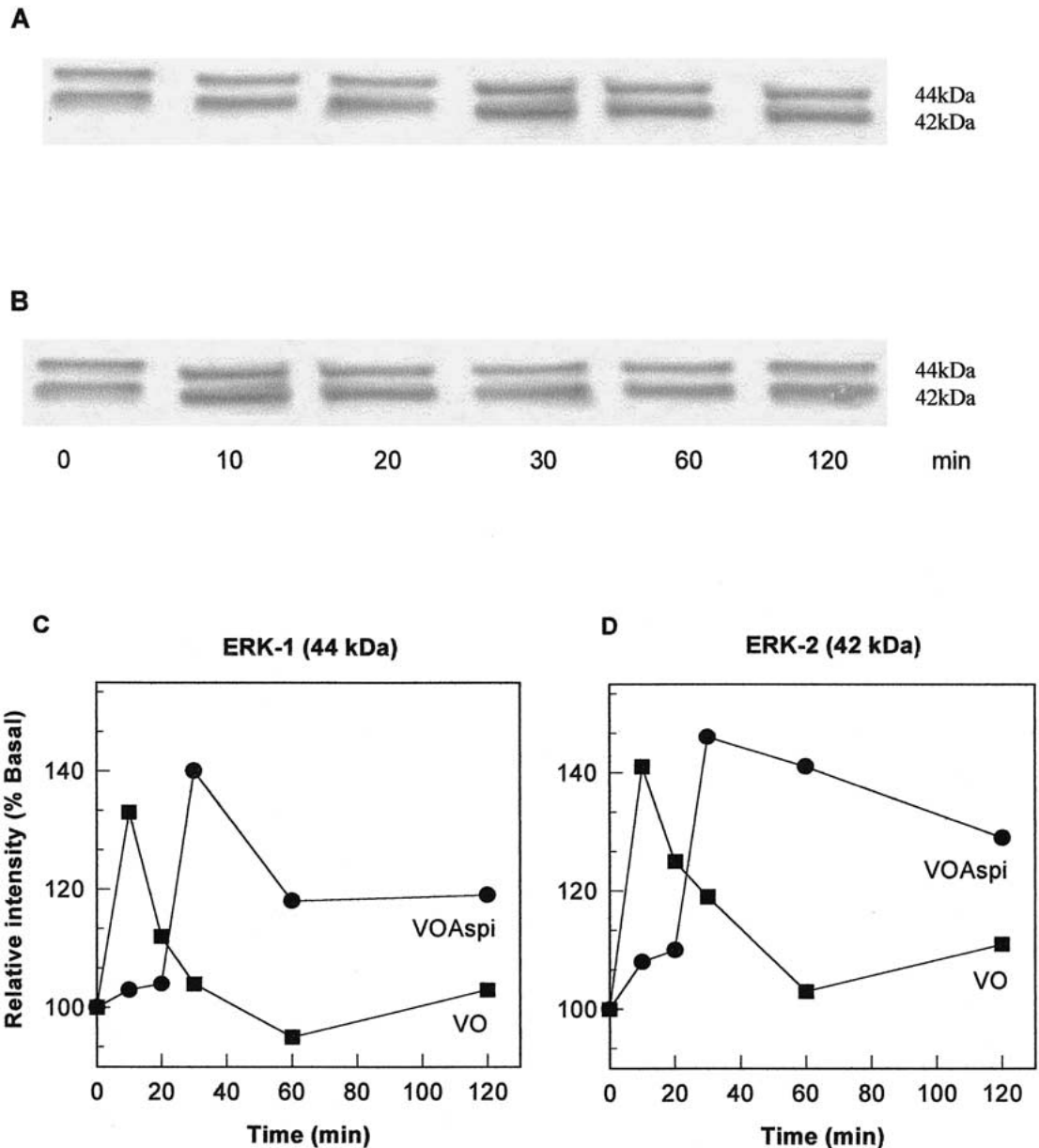


Fig. 5. Kinetics of vanadium effects on Erks expression. UMR106 cells were serum starved for 24 h and then incubated in DMEM with 1 mM VOAspi (A) or 1 mM vanadyl (B) for 0 to 120 min. Cell extracts were separated by 12.5% SDS-PAGE and analyzed by Western blot. Erk-1 (44 kDa band) and Erk-2 (42 kDa band) are indicated in the figures. Images were scanned and analyzed by the Scion-beta 2 program (C and D). The relative intensity of each band is presented as % basal as a function of the incubation time.

of Erks. Maximal stimulation of ERK-1 and -2 was observed between 10 and 20 min (data not shown). VOAspi caused a lower expression of Erks than VO in the range of 0–200 μ M. However, the opposite effect was observed at doses >250 μ M.

All these results demonstrated that VOAspi can induce the Erk signaling pathway in osteoblast-like cells

and suggest that this mechanism may be involved in its bioactivity.

Effect on PTPase activity of osteoblast fraction

Increasing evidence points towards a major role of PTPases in the mechanisms of action of different vanadium compounds (Gresser & Tracey 1990; Huyer

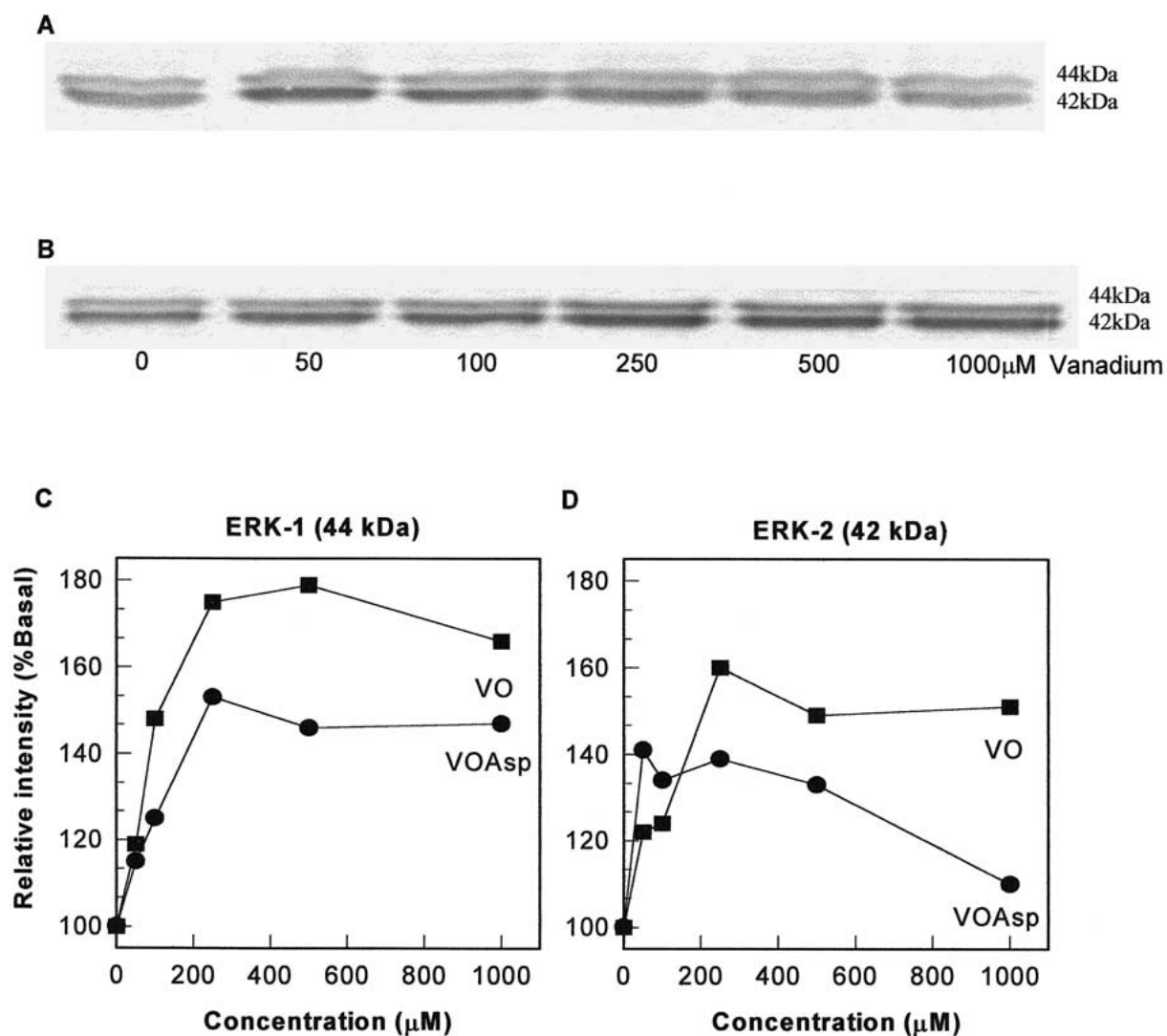


Fig. 6. Dose-response curves of the effect of vanadium compounds on Erks expression. UMR106 cells were serum starved for 24 h and then incubated in DMEM with different doses of VOAspi (A) or vanadyl (B) at 37 °C for 10 min. Western blot of Erk-1 (44 kDa) and Erk-2 (42 kDa) are shown. The relative intensity was analyzed and plotted for VOAspi (C) and vanadyl (D) as % basal, as a function of the vanadium concentration.

et al. 1997). In order to further investigate signaling pathways involved in the new vanadium complex (VOAspi) bioactivity, we studied the effect of VO and VOAspi on the kinetics of inhibition of alkaline and neutral PTPases from cytosol and particulate fractions of osteoblast-like cells.

Figures 7 and 8 show that both compounds inhibited alkaline and neutral PTPases in a dose-response manner. In the cytosolic fraction, the former enzyme was equally inhibited by both vanadium compounds (Figure 7A). At concentrations $<20 \mu\text{M}$ and $>80 \mu\text{M}$, VOAspi was a stronger inhibitor than VO. Contrary,

upon microsomal alkaline PTPase activity, VO caused a stronger effect than VOAspi (Figure 7B).

On the other hand, vanadium compounds were weak inhibitors of neutral PTPases (Figure 8A and B). VO and VOAspi had the same inhibition potency for cytosolic neutral PTPase (Figure 8A), although at low concentrations (5–10 μM), VO proved to be stronger than VOAspi. On the other hand, in the microsomal fraction, VOAspi had a more potent inhibitory effect on the neutral PTPases, reaching a 25–30% inhibition within the 25–100 μM concentration range. A slight

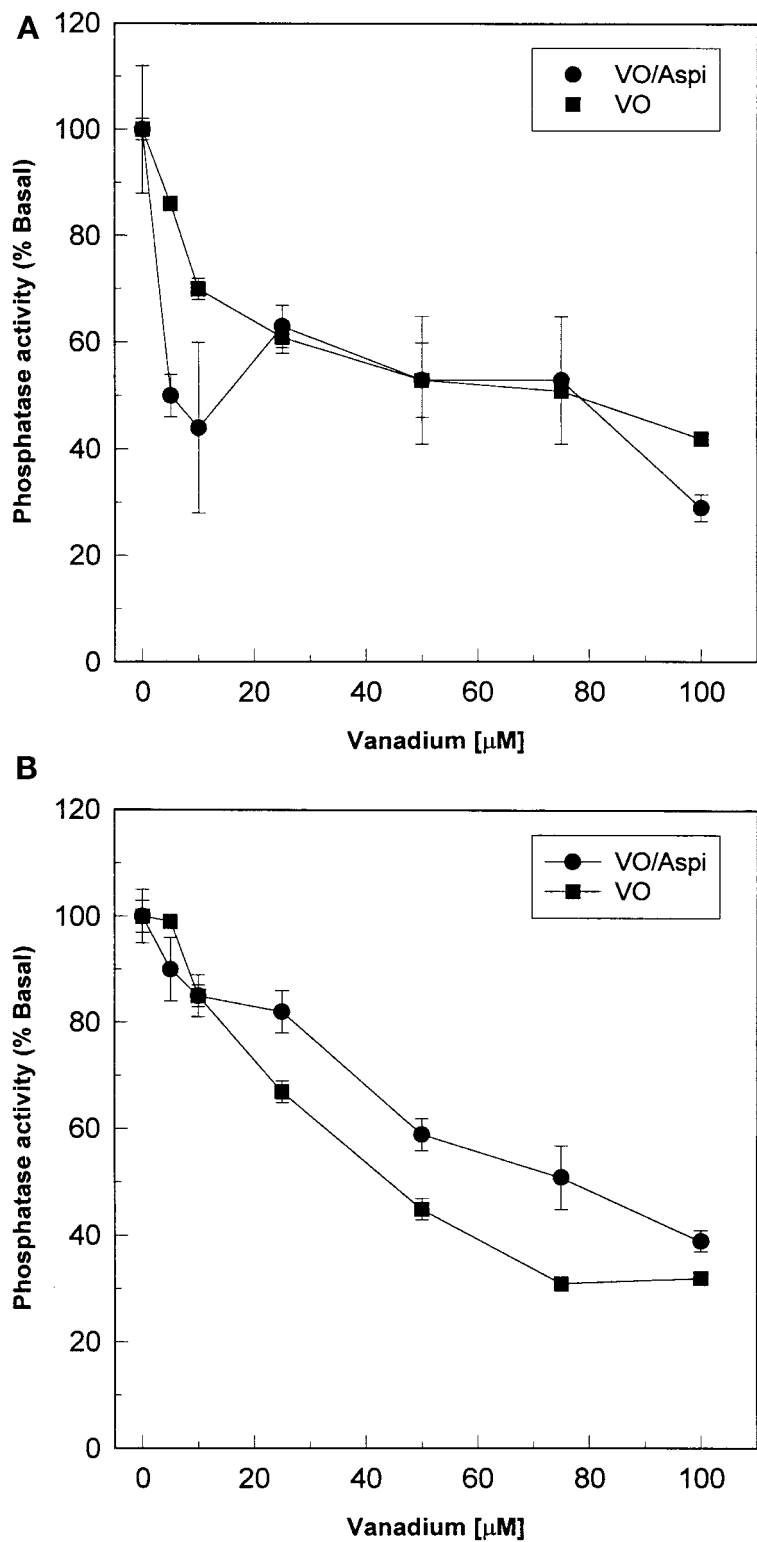


Fig. 7. Effect of vanadium compounds on alkaline PTPase activity in cellular fractions of MC3T3E1 cells. Cytosolic (A) and microsomal (B) fractions were incubated with pNPP in buffer pH 10.5 with different vanadium concentrations, to evaluate alkaline PTPases. Data represent mean \pm SEM, ($n = 8$).

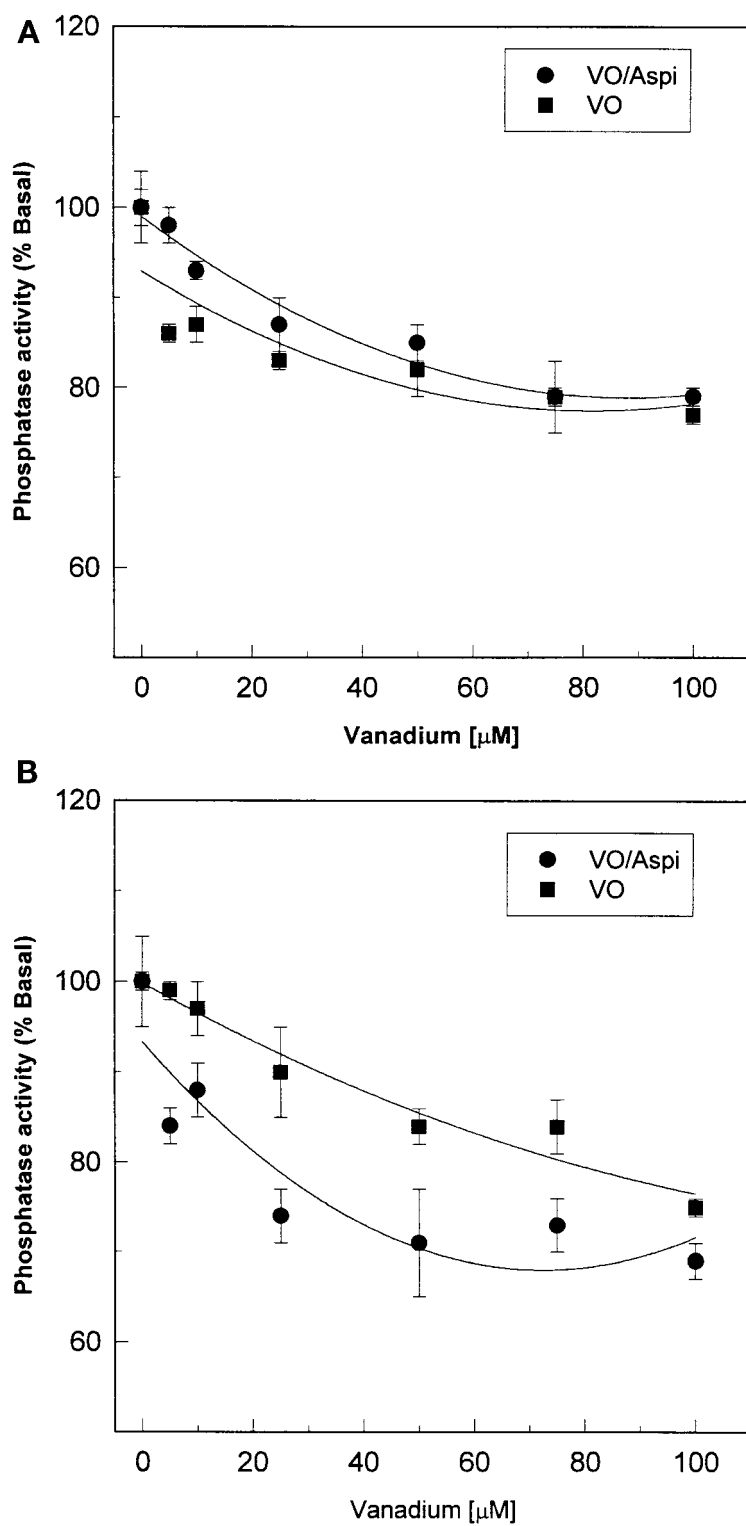


Fig. 8. Effect of vanadium compounds on neutral PTPase activity in cellular fractions of MC3T3E1 cells. To evaluate neutral PTPase, cytosolic (A) and microsomal (B) fractions were incubated with pNPP in buffer HEPES pH 7.5 with different vanadium concentrations. Data represent mean \pm SEM, ($n = 8$).

effect was observed for VO, which attained the 25% of inhibition at a concentration of 100 μM (Figure 8B).

These results demonstrated that PTPases present in osteoblast extracts can be inhibited by VOAspi complex and this may be the mechanism that can activate the tyrosine phosphorylation pathway in osteoblast-like cells.

Vanadium compounds have been widely used as general PTPase inhibitors, although their mechanism of action has not been investigated in detail. For instance, vanadate is a phosphate analog and adopts a trigonal bipyramid structure, similar to that of the transition state of the enzymes participating in the phosphate metabolism (Gresser & Tracey 1990). On the other hand, pervanadates are stronger insulin-mimetic agents and contain one or more chelating ligands in addition to the oxo and peroxy ligands (Posner *et al.* 1994). Recently Huyer *et al.* (1997) have shown that vanadate and pervanadate inhibit PTPases through completely different mechanisms. While vanadate was demonstrated to be a competitive and reversible inhibitor for purified PTP1B, pervanadate irreversibly inhibited this activity by oxidizing a key cysteine. On the other hand, bis(maltolato)-oxovanadium(IV) (BMOV), in which the vanadium atom has a square pyramidal coordination sphere is also a strong PTPase inhibitor (Krejsa *et al.* 1997).

Even though the inhibition of purified PTPases by vanadium(IV) has not been completely investigated, the vanadium(IV) is probably much less potent than vanadium(V). In our study, the PTPase activity assayed at neutral pH in the microsomal fraction seems to be more sensitive to VOAspi than VO (Figure 8B). VOAspi may have a strong affinity for the neutral PTPase present in this fraction. Another possible mechanism involved in the cytotoxic effects could be the generation of oxidative stress. Thus, VOAspi could be a more potent oxidizing agent than VO, entering in a redox-cycling and generating reactive oxygen/nitrogen species. This seems to be the case, since VOAspi was a stronger inductor of lipid peroxidation in both osteoblast cell lines. The evidence suggests that the oxidative stress could be involved in the cytotoxic effect of VOAspi complex when used at high concentrations.

Conclusions

It is well known that vanadium compounds have insulin- and growth factor-mimetic actions in living

organisms and different types of cells in culture. However, they also show toxic effects at high doses or in prolonged administration. Moreover, vanadyl(IV) cation has less toxic effect than vanadium(V), but it is unstable under physiological pH. At present, scientists are highly interested in developing new vanadium derivatives with insulin-mimetic properties and less adverse effects. Special attention is paid to the complexation of vanadyl(IV) cation with organic ligands in order to improve its biodisponibility and beneficial effects.

In the complex $[\text{VO}(\text{aspirin})\text{ClH}_2\text{O}]_2$, the coordination between aspirin and vanadyl(IV) cation takes place through the deprotonated carboxylate groups behaving as bidentated bridging ligands. The acetyl group remains unchanged being this behaviour different from that of other metallic aspirinates. In the suggested structure of the complex, the vanadium atom presents a square pyramidal coordination sphere like in other vanadium compounds (such as BMOV) with similar mimetic properties.

In the osteoblast-like cells, VOAspi exerted more potent cytotoxic effects than VO as assessed by morphological changes, cell survival and lipid peroxidation. These effects may be partially explained through the expression of Erks and the inhibition of the PTPases present in the cellular extracts.

Acknowledgements

The authors thank to Prof. Dr CL Gomez Dumm and Lic. F Riccilo for the pictures of the cells. SBE and EGF are members of the Carrera del Investigador, CONICET, Argentina; AMC and PAMW are members of the Carrera del Investigador, CICIPBA, Argentina. VCS is a fellowship from FOMEC-UNLP, Argentina. DAB is a fellowship from the Colegio de Farmacéuticos de la Provincia de Buenos Aires, Argentina. This work was supported by grants from UNLP, CICIPBA, Agencia de Promoción Científica y Tecnológica (PICT 00375 and PICT 06-06148), CONICET (PIP 1044/98) and Colegio de Farmacéuticos de la Provincia de Buenos Aires, Argentina.

References

- Allegretti Y, Ferrer EG, Gonzales Baró AC, Williams PAM. 2000 Oxovanadium(IV) complexes of quinic acid. Synthesis, characterization and potentiometric study *Polyhedron* **19**, 2613–2619.

- Ballhausen CJ, Gray HB. 1962 The electronic structure of the vanadyl ion 1962 *Inorg Chem* **1**, 111–122
- Baslas RK, Zamani R, Nomani AA. 1979 Studies on the metal-complex of acetyl salicylic acid (aspirin). *Experientia* **35**, 455–456
- Barrio DA, Braziunas MD, Etcheverry SB, Cortizo AM. 1997 Malto complexes of vanadium(IV) and (V) regulate *in vitro* alkaline phosphatase activity and osteoblast-like cell growth. *J Trace Elements Med Biol* **11**, 110–115.
- Binev IG, Stamboliyska BA, Binev YI. 1996 The infrared spectra and structure of acetylsalicylic acid (aspirin) and its oxoanion; an ab initio force field treatment. *J Mol Struct* **378**, 189–197.
- Bradford M. 1976 Rapid and sensitive method for quantification of microgram quantities of protein utilizing the principle of protein-dye binding. *Anal Biochem* **72**, 248–254.
- Brown DH, Smith WE, Teape IW, Lewis AJ. 1980 Antiinflammatory effects of some copper complexes. *J Med Chem* **23**, 729–734.
- Carvill A, Higgins P, McCann M, Ryan H, Shiels A. 1989 Synthesis, Spectroscopic, Electrochemical, and Magnetic Properties of Dimolybdenum(II,II), Diruthenium-(II,III) and -(II,II) Complexes containing Bridging Aspirinate (2-Acetoxybenzoate) Ligands. *J Chem Soc Dalton Trans*, 2435–2442
- Chasteen ND, ed. 1990 *Vanadium in Biological Systems*. Dordrecht, The Netherlands: Kluwer Academic Publishers.
- Clark RJH. 1973 Vanadium. In: Bailar JC, Emeléns HJ, Nyholm Sir R, Trotman-Dickenson AF, eds. *Comprehensive Inorganic Chemistry*. Vol. 3. Oxford: Pergamon Press Ltd; 491–551.
- Cortizo AM, Bruzzone L, Molinuevo S, Etcheverry SB. 2000a A possible role of oxidative stress in the vanadium-induced cytotoxicity in the MC3T3E1 osteoblast and UMR106 osteosarcoma cell lines. *Toxicology* **147**, 89–99.
- Cortizo AM, Caporossi M, Lettieri G, Etcheverry SB. 2000b Vanadate-induced nitric oxide production: role in osteoblast growth and differentiation. *Eur J Pharmacol* **400**, 279–285
- Cortizo AM, Etcheverry SB. 1995 Vanadium derivatives act as growth factor-mimetic compounds upon differentiation and proliferation of osteoblast-like UMR106 cells. *Mol Cell Biochem* **145**, 97–102
- Domingo JL. 2000 Vanadium and diabetes. What about vanadium toxicity? *Mol Cell Biochem* **203**, 185–187.
- Etcheverry SB, Cortizo AM 1998. Bioactivity of vanadium compounds in cells in culture In: Nriagu JO, ed. *Vanadium in the Environment*. **15**. New York: John Wiley & Sons, Inc.; 359–394
- Etcheverry SB, Crans DC, Keramidis AD, Cortizo AM. 1997 Insulin mimetic action of vanadium compounds on osteoblast-like cells in culture. *Arch Biochem Biophys* **338**, 7–14.
- Etcheverry SB, Williams PAM, Barrio DA, Sálice VC, Ferrer EG, Cortizo AM. 2000 Synthesis, characterization and bioactivity of a new VO²⁺/Aspirin complex. *J Inorg Biochem* **80**, 169–171.
- Ferrer EG, Williams PA, Baran EJ. 1993 The interaction of the VO²⁺ cation with oxidized glutathione. *J Inorg Biochem* **50**, 253–262.
- Goldfine AB, Willsky G, Kahn CR. 1998 Vanadium salts in the treatment of human diabetes mellitus. In: Tracey AS, Crans DC, eds. *Vanadium compounds. Chemistry, biochemistry and therapeutic applications* **28**. ACS Symposium series 711. American Chemical Society, Washington, DC, 353–368.
- Gresser MJ, Tracey AS. 1990 Vanadate as phosphate analogs in biochemistry. In: Chasteen ND, ed. *Vanadium in Biological Systems*. The Netherlands: Kluwer Academic Publishers; 63–79.
- Huyer G, Liu S, Kelly J *et al.* 1997 Mechanism of inhibition of protein tyrosine phosphatase by vanadate and pervanadate. *J Biol Chem* **272**, 843–851.
- Krejsa CM, Nadler SG, Esselstyn JM, Kavanagh TJ, Ledbetter JA, Schieven GL. 1997 Role of oxidative stress in the action of vanadium phosphotyrosine phosphatase inhibitors. *J Biol Chem* **272**, 11541–11549.
- Kögerler P, Ferrer EG, Baran EJ. 1996 Preparation and properties of some salts of the Bis(benzylmalonato) aquovanadium(IV) Anion. *Monatsh Chem* **127**, 801–810.
- Laemmli UK. 1970 Cleavage of structural proteins during the assembly of the head of bacteriophage T4. *Ann N Y Acad Sci* **51**, 660–670.
- Lever ABP. 1984 *Inorganic Electronic Spectroscopy*. 2nd edition. Amsterdam: Elsevier.
- Li J, Elberg G, Shechter Y. 1996 Phenylarsine oxide and vanadate: apparent paradox of inhibition of protein phosphotyrosine phosphatases in rat adipocytes. *Biochim Biophys Acta* **1312**, 223–230.
- Lin-Vien, Colthup NB, Fateley WG, Graselli JG 1991 *Infrared and Raman Characteristic Frequencies of Organic Molecules*. San Diego: Academic Press.
- Nakamoto K. 1997 *Infrared and Raman Spectra of Inorganic and Coordination Compounds*. Part B. New York: Wiley.
- Nielsen FH 1995 Vanadium in mammalian physiology and nutrition In: Siegel H, Siegel A, eds. *Vanadium and its role in life* **31**. New York: Marcell Dekker; 543–573.
- Nriagu JO. 1998 History, occurrence and uses of vanadium In: Nriagu JO, ed. *Vanadium in the Environment*. New York: John Wiley & Sons, Inc; 1–24.
- Ohkawa H, Ohishi N, Yagi K. 1979 Assay for lipid peroxides in animal tissues by thiobarbituric acid reaction. *Anal Biochem* **95**, 351–358.
- Pandey SK, Theberge JF, Bernier M, Srivastava AK. 1999 Phosphatidylinositol 3-kinase requirement in activation of Ras/c-Raf-1/Mek/Erk and p70 (s6k) signaling cascade by insulin-mimetic agent vanadyl sulfate. *Biochemistry* **38**, 14667–14675.
- Posner BI, Faure R, Burgess JW *et al.* 1994. Peroxovanadium compounds. A new class of potent phosphotyrosine phosphatase inhibitors which are insulin-mimetics. *J Biol Chem* **269**, 4596–4604.
- Sálice VC, Cortizo AM, Gómez Dumm CL, Etcheverry SB. 1999 Tyrosine phosphorylation and morphological transformation induced by for vanadium compounds on MC3T3E1. *Mol Cell Biochem* **198**, 119–128.
- Shechter Y. 1990 Insulin-mimetic effect of vanadate. Possible implications for future treatment of diabetes. *Diabetes* **39**, 1–5.
- Sorenson IR. 1982 The anti-inflammatory activities of copper complexes. In: Siegel H, ed. *Metal Ions in Biological Systems* **14**. New York: Marcel Dekker; 77–124.
- Srivastava AK, Chiasson J-L eds. 1995 Vanadium compounds: Biochemical and therapeutic Applications. Focused issue in *Mol Cell Biochem* **153**.
- Stern A, Yin X, Tsang S-S, Davison A, Moon T. 1993 Vanadium as a modulator of cellular regulatory cascades and oncogene expression. *Biochem Cell Biol* **71**, 103–112
- Syamal A. 1975 Spin – spin coupling in oxovanadium(IV) complexes. *Coord Chem Rev* **16**, 309–339.
- White MF, Kahn CR. 1994 The insulin signaling system. *J Biol Chem* **269**, 1–4.
- Williams PAM, Kögerler P, Baran EJ. 1998 Interaction of the VO²⁺ cation with suprofen. *Acta Farm Bonaerense* **17**: 31–34